Experimental Thermal and Fluid Science 60 (2015) 213–222

Contents lists available at ScienceDirect

Experimental Thermal and Fluid Science

journal homepage: www.elsevier.com/locate/etfs

Measurements of skin friction and heat transfer beneath an impinging slot jet

M. Baris Dogruoz [a], Alfonso Ortega [b,*], Russell V. Westphal [c]

[a] Cisco Systems Inc., San Jose, CA 95134, USA
[b] Department of Mechanical Engineering, Villanova University, Villanova, PA 19085, USA
[c] Department of Mechanical Engineering, California Polytechnic State University, San Luis Obispo, CA 93407, USA

ARTICLE INFO

Article history:
Received 28 April 2014
Received in revised form 2 August 2014
Accepted 31 August 2014
Available online 8 September 2014

Keywords:
Slot jet
Skin friction
Stanton gauge
Oil film interferometry
Heat transfer
Secondary maxima

ABSTRACT

An experimental study was performed to measure skin friction and surface heat transfer for an orthogonal slot jet impinging on a flat plate. Surface pressure, total pressure, velocity profiles, skin friction and temperature distributions were obtained within twenty nozzle widths of jet centerline at a range of $20,000 < Re_j < 36,000$. Stanton gauge, and oil film methods were used to measure skin friction. Multiple micro-thermocouples attached to an iso-flux surface were utilized to acquire the target plate temperature distribution. The majority of the experimental data was taken at a nozzle-to-plate spacing of four nozzle widths where the jet was still within its potential core length. The local surface heat transfer and skin friction distributions showed local extrema that were not coincident, and whose behavior do not appear to be entirely consistent with hypotheses that attribute the secondary peak to laminar-to-turbulent transition of the surface layer. It is believed that these off center peaks occur as a consequence of enhanced turbulent momentum and heat transport in the wall-normal direction.

1. Introduction

A high aspect ratio rectangular impinging jet, often referred to as a slot jet in the literature, leads to a wall-bounded jet flow developing from a stagnation line with strong acceleration due to rapid turning for a distance of a few jet widths. This is illustrated in Fig. 1. The skin friction rises rapidly from stagnation, reaching a peak at a location which is nearly that of the peak favorable pressure gradient as well. The wall heat transfer profile displays a broad peak centered at the stagnation line. The peak values of skin friction and surface heat transfer in the region near stagnation are the basis for impingement cleaning and cooling processes. Beyond this region within a distance of about two nozzle widths from the stagnation line, where strong gradients in pressure, surface heat transfer, and skin friction are observed, the wall-bounded flow develops as a constant-pressure wall jet.

The hydrodynamic and thermal characteristics of impinging jets have been extensively reviewed [1–5]. Downs and James [1] reviewed round and slot turbulent impinging jets. They surveyed geometry, temperature, crossflow, turbulence level, incidence, curvature and nozzle exit effects on stagnation and local heat transfer coefficients. Jambunathan et al. [2] reviewed the heat transfer data for single circular impinging jets in the range of $5000 < Re_j < 124,000$ and $1.2 < H/D < 16$. They also presented a comprehensive correlation to determine local heat transfer coefficients for round jets. Martin [3] presented empirical correlations of heat and mass transfer of impinging jets issued from single or arrays of slot, circular and specialty nozzles. A design methodology for high performance arrays of nozzles to enhance heat transfer on target surfaces was also shown. Viskanta [4] presented a review of isothermal gas and flame impinging jets for single and arrays of jets for almost all the possible cases encountered in relevant industrial applications. Similar to [1], Viskanta [4] surveyed the effects of several parameters such as turbulence, entrainment, nozzle exit conditions, and curvature on the heat transfer behavior. Zuckerman and Lior [5] presented a review of jet physics, numerical modeling and an updated list of heat and mass transfer correlations shown elsewhere [3] for single phase impinging jets. They investigated turbulence generation and its effects on the off-center peaks for several different geometries and Reynolds number intervals. A detailed description and comparison of various turbulence models, near-wall modeling in computing jets was also presented.

Tu and Wood [6] conducted an experimental study to predict the wall shear stress due to a turbulent impinging slot jet by using Stanton gauge and Preston tube techniques. In a range of $3040 \leqslant Re_j \leqslant 11,000$, they showed that the pressure distribution has a

* Corresponding author. Tel.: +1 (610) 519 7440.
E-mail addresses: bdogruoz@cisco.com (M.B. Dogruoz), alfonso.ortega@villanova.edu (A. Ortega), rvwestph@calpoly.edu (R.V. Westphal).

http://dx.doi.org/10.1016/j.expthermflusci.2014.08.014
0894-1777/© 2014 Published by Elsevier Inc.

Nomenclature

A_s	total surface area of the heated foil (m^2)
B	velocity gradient in an accelerating boundary layer (s^{-1})
c_f	skin friction coefficient, $\tau_w / (0.5\rho u_j^2)$ (dimensionless)
c_p	pressure coefficient, $(P - P_\infty) / (0.5\rho u_j^2)$ (dimensionless)
D	nozzle diameter for circular jets or hydraulic diameter for slot jets ($D = 2W$) (m)
h	heat transfer coefficient, $q_c/[A_s(T_w - T_j)]$ (W/m^2 K)
H	nozzle-to-plate distance (m)
k_f	thermal conductivity of the cooling fluid (W/m K)
Nu	Nusselt number, $Nu = hD/k_f$ (dimensionless)
P	static pressure (Pa)
P_∞	ambient pressure (Pa)
Pr	Prandtl number, $Pr = \nu/\alpha$ (dimensionless)
q_c	rate of heat transfer convected through the surface (W)
Re_j	jet Reynolds number, $Re_j = (\rho v_j D)/\mu$ (dimensionless)
T	temperature (K)
u	velocity in the streamwise direction (m/s)
v	velocity in the wall-normal direction (m/s)
$V_{cl,j}$	jet centerline ($x = 0$) velocity at the nozzle-exit ($y_j = 0$) (m/s)
W	nozzle width (m)
x	streamwise coordinate (m)
y	wall-normal coordinate (m)
y_j	axial distance from the nozzle exit ($H - y$) (m)

Subscripts

j	nozzle exit
w	wall

Superscripts

$\cdot'$	fluctuating component
$\bar{\cdot}$	mean component

Greek symbols

α	thermal diffusivity (m^2/s)
δ	uncertainty
Δ	boundary layer thickness (m)
μ	absolute viscosity (Pa s)
ν	dynamic viscosity (m^2/s)
τ	shear stress (N/m^2)

Gaussian profile that is independent of Re_j up to $H/W = 12$. For a similar geometry and at a higher velocity ($Re_j = 90{,}000$), experimental data by Guo and Wood [7] showed a secondary peak and this was attributed to transition from a laminar flow regime to a turbulent flow regime. Phares et al. [8] also observed these secondary peaks in the case of circular jets and also attributed the occurrence of these secondary maxima to laminar-to-turbulent transition. Ortega et al. [9] used Stanton gauge, Preston tube, and oil film methods to measure the skin friction due to a slot impinging jet at $Re_j = 36{,}000$ and $H/W = 4$. In contrast to [6–8], taking also the heat transfer data into account, they concluded that the secondary maxima could not be attributed to the laminar-to-turbulent transition, however an explanation for those secondary peaks was not provided. Other experimental studies investigating wall shear stress due to impinging slot jets [10,11] used the hot film surface probe technique and showed that the Reynolds analogy is not valid for this particular flow.

Singer and Ortega [12] conducted measurements on an isoflux surface at various Reynolds numbers and jet heights for slot jets. It was demonstrated that the Nusselt number distributions for $H/W = 2, 4$ show secondary peaks when $Re_j \geqslant 15{,}000$. Cadek [13] performed a similar study on an isothermal surface at a range

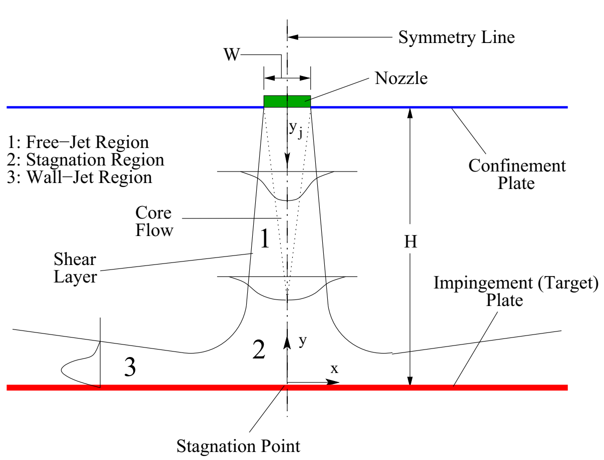

Fig. 1. Schematic and flow field of a typical impinging jet.

of $9300 < Re_j < 224{,}600$ and $H/W = 2$–16 with various nozzle widths. van Heiningen [14] reported experimental and numerical results of impingement heat transfer on isothermal surfaces for fully confined slot jets for a range of Re_j at $H/W = 2.6$ and 6.0. Although the magnitude of Nusselt number is different, the data from [13,14] showed a similar behavior to that of [12].

Results for $Re_j < 10{,}000$ and $H/W > 6$ did not show secondary peaks in the Nusselt number distribution [12,15–17]. While the circular jet data of [15] does not show any change in the location of the off center peak with velocity, an intriguing aspect of the slot jet data reported for $H/W = 4$ [12,16,17] is that the location of the second peak in Nusselt number moves *farther* from the stagnation area with increasing Re_j. While there was no explanation of the secondary peaks in the former two studies, the latter attributed the secondary peaks to laminar-to-turbulent transition where the turbulence level around the stagnation area was still considerable especially in the case of $H/W = 2, 4$ and higher jet velocities. It might instead have been expected that increasing the Reynolds number would yield transition closer to the stagnation line. Thus, one of the motivating questions for the present study is the following: *if transition were predominantly responsible for the secondary peak, why did this peak move farther from instead of closer to the stagnation line as Reynolds number increased?*

Detailed measurements of pressure, skin friction, velocity and heat transfer in impinging slot jets are sparse at moderately high Reynolds numbers and nozzle-to-plate spacings less than the jet potential core lengths, $H/W < 5$–6. The present study was undertaken to acquire detailed information on surface pressure, skin friction, velocity profile, heat transfer of an unconfined impinging slot jet within its potential core, and further investigate the behavior of the off-center peaks in the shear stress and heat transfer distributions over a range of jet velocities and nozzle-to-plate spacings.

2. Experimental setup and procedure

2.1. Slot jet facility

The slot jet was produced by the 6.35 mm wide by 152.4 mm long (24:1 aspect ratio) exit of a 24:1 contraction fitted with flow conditioning and supplied by a variable-speed centrifugal blower